Ferroelectric Liquid Crystal Pixel Arrays with 1 × 1-μm Pixel Pitch for Electro-Holography

Shintaro Aso[1], Ken-ichi Aoshima[1], Ryo Higashida[1], Nobuhiko Funabashi[1], Junichi Shibasaki[1], Takahiro Ishinabe[2], Yosei Shibata[2], Hideo Fujikake[2], Kenji Machida[1]

asou.s-iy@nhk.or.jp
[1]NHK, 1-10-11 Kinuta, Setagaya-ku, Tokyo 157-8510, Japan
[2]Tohoku University, 6-6-05 Aoba, Aramaki, Aoba-Ku, Sendai, Miyagi 980-8579, Japan
Keywords: Holographic Display, Spatial Light Modulator, Ferroelectric Liquid Crystal

ABSTRACT

We fabricated ferroelectric liquid crystal pixel arrays with small pixel pitch of 1 × 1 μm using a prepatterned two-layer electrode and investigated the light modulation properties. Furthermore, we obtained reconstructed three-dimensional holographic images with a wide viewing-zone angle using a 10k × 10k array with 1 × 1-μm pixels.

1 INTRODUCTION

Holography is the ultimate three-dimensional (3D) display technology because it can precisely reconstruct the light emitted from an object [1, 2]. It satisfies all the conditions necessary for autostereoscopic vision, such as motion parallax, binocular disparity, vergence, and accommodation. Although it has great potential for 3D images, it requires a display device with very high performance, such as an extremely small pixel pitch of 1 μm, for realizing a practically sufficient viewing-zone angle of a reconstructed holographic image. Liquid crystal (LC) spatial light modulators (SLMs) have been widely used in holographic displays because of their large amplitude- and phase-modulation capabilities [3-5]. Recently, LC-SLMs with small pixel pitch for electro-holography has been actively researched [4, 5]. An LC-SLM with a pixel pitch of 3.015 μm for a holographic head-mounted display was developed for practical use [4]. Moreover, an LC-SLM with a pixel pitch of 1 × 9 μm was reported; however, its LC light modulation properties have not been described in detail [5]. For realizing an LC-SLM with very small pixel pitch, it is crucial to reduce crosstalk between adjacent pixels. Therefore, a dielectric wall structure between LC pixels has been proposed [6, 7]. This structure suppresses electric field leakage and prevents the penetration of the elastic force of the LC from adjacent pixels, realizing the individual driving of 1-μm-pitch LC pixels. Further, in a study using simple stripe electrodes, a one-dimensional, 1-μm-pitch ferroelectric LC (FLC) device achieved higher resolution than that of a nematic LC without the wall structure. This advantage of the FLC device is attributed to the difference in the LC driving methods [8]. In nematic LC devices, the ON- and OFF-state pixels are controlled by the presence or absence of a driving voltage of the pixel electrodes; in contrast, in FLC devices, the ON- and OFF-state pixels are controlled by the difference in the polarity of the driving voltages. This means the directions of FLC molecules in both ON- and OFF-state pixels are fixed by the driving voltages. Therefore, OFF-state pixels in FLC devices are less affected by the leakage electric field from the ON-state pixels. However, for two-dimensional (2D) FLC devices with small pixel pitch (about 1 × 1 μm), which is essential for full-parallax holographic images, the effect of the 2D-distributed in-plane leakage electric field on the high-resolution properties has not been examined. In this study, we developed FLC pixel arrays driven by a separated two-layer electrode. Thus, we realized a 2D LC-array without cell selection transistors. We also examined the 2D high-resolution properties of the FLC pixel arrays with a small pixel pitch of 1 × 1 μm. Further, we obtained reconstructed 3D holographic images with a wide viewing-zone angle using a 10k × 10k FLC pixel array with a 1 × 1-μm pixel pitch.

2 EXPERIMENTAL METHOD

To analyze the 2D high-resolution properties of the FLC, we used FLC pixel arrays driven by a pre-patterned two-layer electrode. Figs. 1 and 2 show the structure of the fabricated FLC pixel array. Fig. 1 shows the schematic illustration of the perspective view, and Fig. 2 provides a cross-sectional view of the FLC pixel array. The two-layer electrode is transparent and has a lower and an upper layer of indium-zinc-oxide (IZO) (20 nm), and a SiO_2 insulation layer (320 nm). The upper-layer electrode has square apertures with a checkered pattern. The aperture dimensions were 0.8 × 0.8 μm with a pixel pitch of 1 × 1 μm. Furthermore, rectangular apertures of dimensions 0.8 × 1.8 μm with a pixel pitch of 1 × 2 μm were also formed to investigate the effect of difference in LC alignment directions on light modulation properties. Alignment films (AL-1254; JSR Co.) were spin-coated on the patterned and common electrodes, and a rubbing treatment was applied to achieve an anti-parallel LC alignment. A 1-μm-thick layer of FLC mixture was sealed between the two-layer electrode and a counter transparent common electrode. Fig. 3 shows the finite element calculation result of the electric potential distribution of an FLC pixel array with 1 × 1-μm pixel pitch. As shown in this figure, we applied +9.0 V to the lower-layer electrode and -1.0 V to the upper-layer electrode of the two-layer electrode, and the common electrode was maintained at 0 V. The relative permittivity of the FLC layer and that of the insulating layer were assumed as 10 and 4.0, respectively. The electric potential at the interface between the two-layer electrode and the FLC layer was -1.0 V in the upper-layer electrode and around +1.5 V at the center of the aperture of the upper-layer electrode. Thus, the 2D FLC pixel array was driven by the spatially distributed positive and negative voltages.

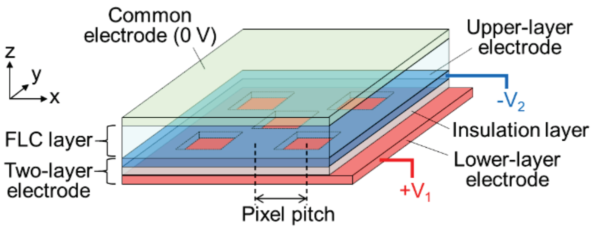

Fig. 1 Schematic illustration of the perspective view of a fabricated ferroelectric liquid crystal (FLC) pixel array

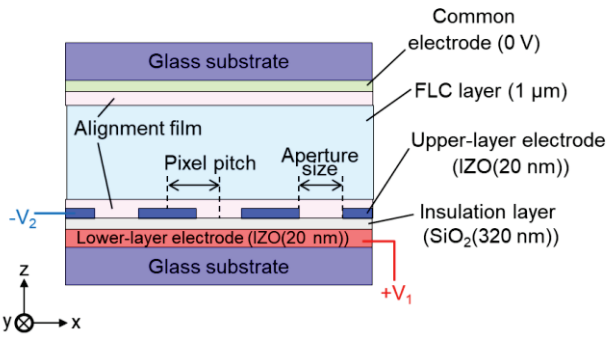

Fig. 2 Cross-sectional view of a fabricated FLC pixel array

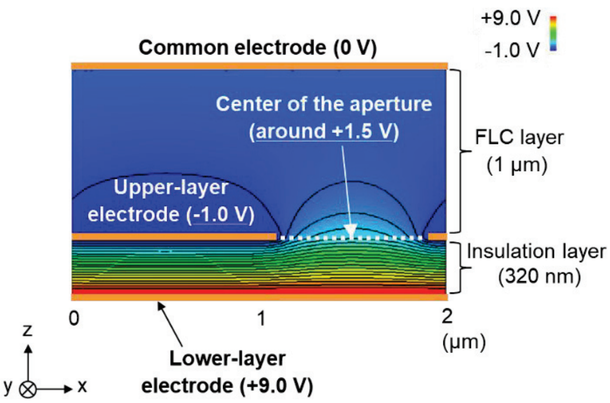

Fig. 3 Finite element calculation result of the electric potential distribution of a 1 × 1-μm pixel pitch of an FLC pixel array

3 RESULTS AND DISCUSSION

3.1 Light Modulation Properties of the 2D FLC Pixel Arrays

Fig. 4 shows the polarizing micrograph of a fabricated FLC pixel array with a pixel pitch of 1 × 1 μm. The direction of the polarizer was 22.5° counterclockwise from the y-axis, and the analyzer was orthogonal to the polarizer. The LC alignment direction was parallel to the y-axis. We applied +9.0 V to the lower-layer electrode and -1.0 V to the upper-layer electrode of the two-layer electrode, and the common electrode was maintained at 0 V. As shown in the figure, a checkered pattern with a pitch of 1 × 1-μm was successfully realized. From this result, we concluded that FLC realizes individual pixel driving in a 2D array with an extremely small pitch of 1 × 1 μm. Thus, the FLC pixel array demonstrated the potential for use in electro-holographic displays with a wide viewing-zone angle of over 36° at a light source wavelength of 633 nm.

We also investigated the performance of rectangular pixels with different LC alignment directions to understand the effect of alignment on light modulation properties, since the rectangular pixels may allow larger area for cell selection transistors on a backplane which also have difficulty to satisfy sufficient performance within a small area. Fig. 5 shows the photomicrograph of a two-layer electrode with a pixel pitch of 1 × 2 μm. The upper layer electrode had apertures of dimensions 0.8 × 1.8 μm. For each pixel, the side along the y-axis was longer than that along the x-axis.

Fig. 6 shows the polarizing micrographs of the FLC pixel arrays with a pixel pitch of 1 × 2 μm with different alignments. These pixel arrays were fabricated with identically designed two-layer electrodes, as shown in Fig. 5; the voltages applied to each electrode were identical to those applied to the 1 × 1 μm pixel array. For the pixel array shown in Fig. 6(a), the alignment direction was parallel to the x-axis (x-axis alignment), while for the pixel array shown in Fig. 6(b), the alignment direction was parallel to the y-axis (y-axis alignment). The x-direction width of the white pixel shown in Fig. 6(b) is greater than that shown in Fig. 6(a). The pixel shape shown in Fig. 6(a) is almost identical to the electrode shape shown in Fig. 5, indicating the white pixel in Fig. 6(b) is elongated to x-direction compared to designed width.

The difference of the white pixel shape between the pixel with the x-axis alignment and the y-axis alignment is attributed to the angle between the direction of the FLC cone axis and the major direction of in-plane electric field from the adjacent pixels. For the rectangular electrode shown in Fig. 5, x-direction electric field from the adjacent pixels is larger than y-direction field since the pixel pitch of the x-direction is smaller than that of the y-direction. Fig. 7 shows a schematic top view of the relationship between the FLC switching directions and the alignment directions. This figure clarifies the response of the electric dipoles of FLC molecules with the x- and y-axis alignment to the in-plane electric field. The electric dipole moments of FLC molecules move along tangential direction to the cone circle. So, when the FLC cone axis is perpendicular to the direction of in-plane electric field (x-axis direction), as shown in Fig. 7(b), the interaction between the dipole moments and the in-plane electric field causes rotation of the FLC molecules. On the other hand, as shown in Fig. 7(a), if the FLC cone axis is parallel to the in-plane electric field, the electric field cannot rotate the dipole moments of the FLC because the dipoles move within the tangential direction to the cone circle and cannot move beyond the cone circle. Since the FLC cone axis is parallel to the x-axis direction when the alignment is x-axis, the width of the white pixel does not expand (Fig.6(a)) along the x-direction, while the width of the white pixel expands (Fig.6(b)) along the x-direction with the y-axis alignment because the FLC cone axis is perpendicular to the x-direction. Therefore, when an SLM has small-pitch rectangular FLC pixels, the FLC cone axis should be oriented in the direction with a smaller pixel pitch to suppress crosstalk between adjacent pixels.

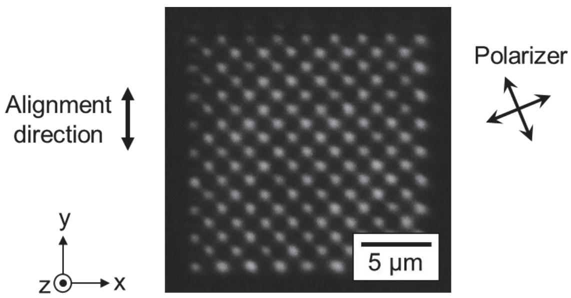

Fig. 4 Polarizing micrograph of a fabricated FLC pixel array with a pixel pitch of 1 × 1 μm

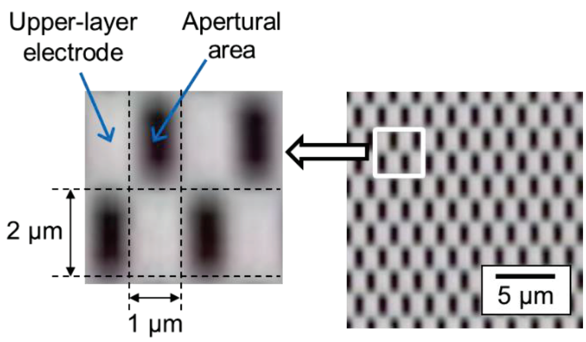

Fig. 5 Photomicrograph of a two-layer electrode with a pixel pitch of 1 × 2 μm

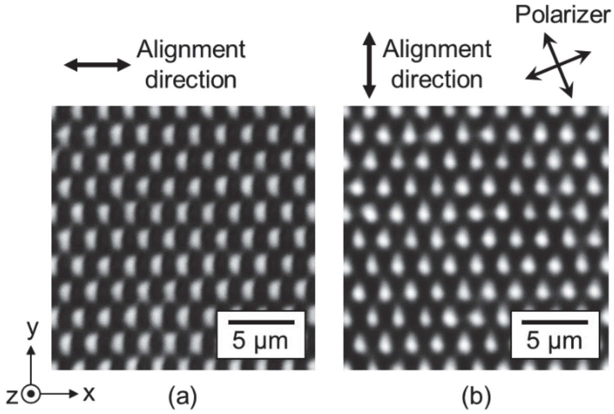

Fig. 6 Polarizing micrographs of the FLC pixel arrays with a pixel pitch of 1 × 2 μm with different alignment directions: (a) x-axis and (b) y-axis alignment

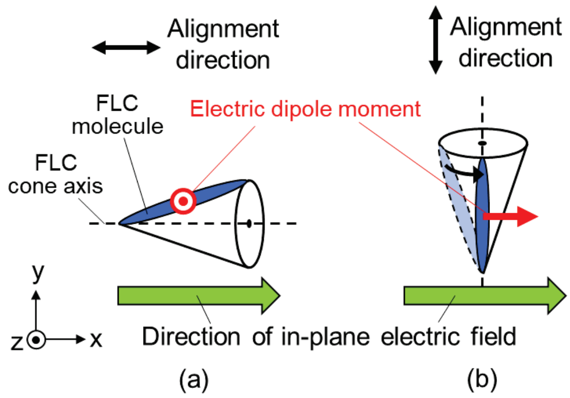

Fig. 7 Responses to the in-plane electric field of the FLC with different alignment directions: (a) x-axis and (b) y-axis alignment

3.2 Reconstruction of a Hologram Using an FLC Pixel Array of 10k × 10k with a Pixel Pitch of 1 × 1 μm

To demonstrate the holographic image reconstruction using an FLC array with a 1 × 1-μm pitch, we fabricated a 10k × 10k array whose aperture pattern in the upper-layer electrode was a binary computer-generated hologram. The structure of the pixel array was identical to that of the checkered pattern array except that we used an Si substrate with a lower-layer Ru electrode to design the pixel array as a reflection-type modulator. Fig. 8 shows the optical setup of the reconstruction of the hologram. A He-Ne laser beam was expanded by a beam expander and introduced into the FLC array through a polarizer with a polarization direction of 112.5° (clockwise direction) from the y-axis. Modulated light in the FLC array was observed from various angles by a CMOS image sensor with an analyzer that was orthogonal to the polarization direction of the incident light. The FLC array was placed at an angle of 9° from the y-axis to the z-axis to prevent the zero-order diffraction light from entering the CMOS image sensor. (This tilt angle of 9° is not shown in Fig. 8.) Fig. 9 shows the holographic images observed upon application of -1.1 V to the upper-layer electrode, +4.7 V to the lower-layer electrode, and 0 V to the common electrode. The 3D holographic images of a Japanese character were reconstructed with a wide viewing-zone angle by using the 1 × 1-μm-pitch FLC array; however, the holographic images became darker at the negative angles. At present, investigation of the dependence of the viewing angle characteristics on the polarization directions of the incident and diffracted light is ongoing. We will evaluate the viewing angle characteristics by LC birefringence simulation for incident and diffracted light to find a solution to improve the viewing angle characteristics.

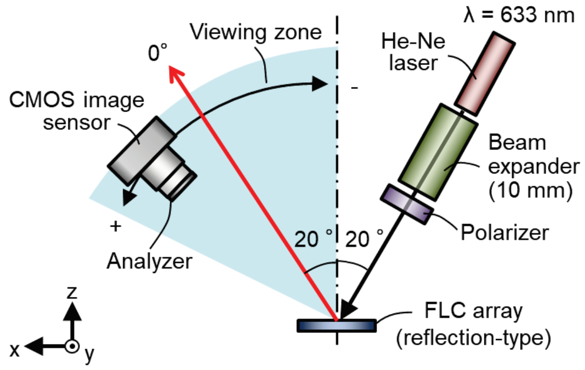

Fig. 8 Optical setup of the reconstruction of the hologram

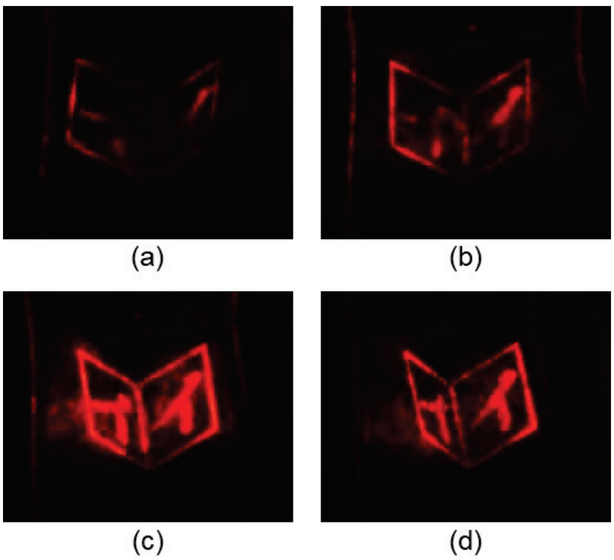

Fig. 9 Reconstructed holographic images observed from various angles: (a) -15°, (b) -6°, (c) +6°, and (d) +15°

4 SUMMARY

We showed that 2D FLC pixel arrays of extremely small pitch (up to 1× 1 μm) have high resolution display capability. To suppress crosstalk between adjacent pixels, the FLC cone axes should be oriented in the direction of the smaller pixel pitch for rectangular pixels. Furthermore, we demonstrated the reconstruction of 3D holographic images with a wide viewing-zone angle using a 10k × 10k FLC array with a pixel pitch of 1 × 1 μm. We showed that the FLC pixel arrays are a strong candidate for realizing a full-parallax holographic display.

ACKNOWLEDGEMENTS

We would like to thank Dr. Yoshitomo ISOMAE, a former student of Tohoku University, for fabricating the FLC layer.

REFERENCES

[1] D. Gabor, “A new microscopic principle,” Nature, Vol. 161, No. 4098, pp. 777-778 (1948).

[2] E. N. Leith and J. Upatnieks, “Reconstructed wavefronts and communication theory,” J. Opt. Soc. Am., Vol. 52, No. 10, pp. 1123-1130 (1962).

[3] N. Hashimoto, S. Morokawa and K. Kitamura, “Real-time holography using the high-resolution LCTV-SLM,” Proc. SPIE 1461, Practical Holography V, pp. 291-302 (1991).

[4] A. K. Abeeluck, A. Iverson, H. Goetz and E. Passon, “High-performance displays for wearable and hud applications,” SID 2018 Digest, pp. 768-771 (2018).

[5] C. S. Hwang, J. H. Choi, J. E. Pi, J. H. Yang, G. H. Kim, Y. H. Kim, J. Y. Kim, W. J. Lee, H. O. Kim, H. K. Lee, M. Y. Kim and J. Kim, “1μm pixel pitch spatial light modulator panel for digital holography,” SID 2020 Digest, pp. 297-300 (2020).

[6] Y. Isomae, Y. Shibata, T. Ishinabe and H. Fujikake, “Experimental study of 1-μm-pitch light modulation of a liquid crystal separated by dielectric shield walls formed by nanoimprint technology for electronic holographic displays,” Opt. Eng., Vol. 57, No. 6, pp. 061624 (2018).

[7] Y. Isomae, T. Ishinabe, Y. Shibata and H. Fujikake, “Alignment control of liquid crystals in a 1.0-μm-pitch spatial light modulator by lattice-shaped dielectric wall structure,” J. Soc. Inf. Display., Vol. 27, pp. 251-258 (2019).

[8] Y. Isomae, S. Aso, J. Shibasaki, K. Aoshima, K. Machida, H. Kikuchi, T. Ishinabe, Y. Shibata and H. Fujikake, “Superior spatial resolution of surface-stabilized ferroelectric liquid crystals compared to nematic liquid crystals for wide-field-of-view holographic displays,” Jpn. J. Appl. Phys., Vol. 59, No. 4, pp. 040901 (2020).